

¹ The Morphological Diversification of Siphonophore Tentilla

³ Alejandro Damian-Serrano^{1,‡}, Steven H.D. Haddock², Casey W. Dunn¹

⁴ ¹ Yale University, Department of Ecology and Evolutionary Biology, 165 Prospect St.,
⁵ New Haven, CT 06520, USA

⁶ ² Monterey Bay Aquarium Research Institute, 7700 Sandholdt Rd., Moss Landing, CA
⁷ 95039, USA

⁸ [‡] Corresponding author: Alejandro Damian-Serrano, email: alejandro.damianserrano@
⁹ yale.edu

¹⁰ Abstract

¹¹ Siphonophore tentilla (tentacle side branches) are unique biological structures for prey capture,
¹² composed of a complex arrangement of cnidocytes (stinging cells) bearing different types
¹³ of nematocysts (stinging capsules) and auxiliary structures. Tentilla present an exuberant
¹⁴ morphological diversity of form and function across species. While associations between
¹⁵ tentilla form and diet have been reported, the evolutionary history giving rise to this
¹⁶ morphological diversity is largely unexplored. Here we explore the evolutionary gains and
¹⁷ losses of novel tentillum substructures and nematocyst types on the most recent siphonophore
¹⁸ phylogeny. Tentilla have a precisely coordinated high-speed strike mechanism of synchronous
¹⁹ unwinding and nematocysts discharge. Here we characterize the kinematic diversity of this
²⁰ prey capture reaction using high-speed video and find relationships with morphological
²¹ characters. Since tentillum discharge occurs in synchrony across a broad morphological
²² diversity, we evaluate how phenotypic integration is maintaining character correlations across
²³ evolutionary time. Moreover, we analyze the dimensionality of the tentillum morphospace,
²⁴ identify instances of heterochrony and morphological convergence, and generate hypotheses
²⁵ on the diets of understudied siphonophore species. Our findings indicate that siphonophore

26 tentilla are phenotypically integrated structures with a complex evolutionary history leading to
27 a phylogenetically structured diversity of forms which are predictive of kinematic performance
28 and feeding habits.

29 **Keywords**

30 Siphonophore, tentilla, nematocysts, character evolution

31 **Introduction**

32 Siphonophores have fascinated zoologists for centuries for their extremely subspecialized
33 colonial organization and integration. Today we hold more knowledge than ever on the
34 morphological diversity of this group due to the extensive work of siphonophore taxonomists
35 in the past few decades (1–10), which has been elegantly synthesized in detailed synopsis (11).
36 In addition, recent advances in phylogenetic analyses of siphonophores (13, 14) have provided
37 a macroevolutionary context to interpret this diversity. With these assets in hand, we can
38 now begin to study siphonophores from an orthogonal perspective, focusing on the diversity
39 and evolutionary history of specific structures. Here we focus on one of such structures: the
40 tentilla. Like many cnidarians, siphonophore tentacles bear side branches (tentilla) with
41 nematocysts. But unlike other cnidarians, most siphonophore tentilla are dynamic structures
42 that react to prey encounters by shooting the nematocyst battery to slap around the prey.
43 This maximizes the surface area of contact between the nematocysts and the prey they fire
44 upon. In addition, siphonophore tentilla present a remarkable diversity of morphologies, sizes,
45 and nematocyst complements (Fig. 1). Our overarching aim is to organize all this phenotypic
46 diversity in a phylogenetic context, and identify the evolutionary processes that generated it.

47 In (14), we collected the most extensive morphological dataset on siphonophore tentilla
48 and nematocysts using state-of-the-art microscopy techniques, and expanded the taxon
49 sampling of the phylogeny to disentangle the evolutionary history. The analyses we carried
50 out led to novel, generalizable insights into the evolution of predatory specialization. The

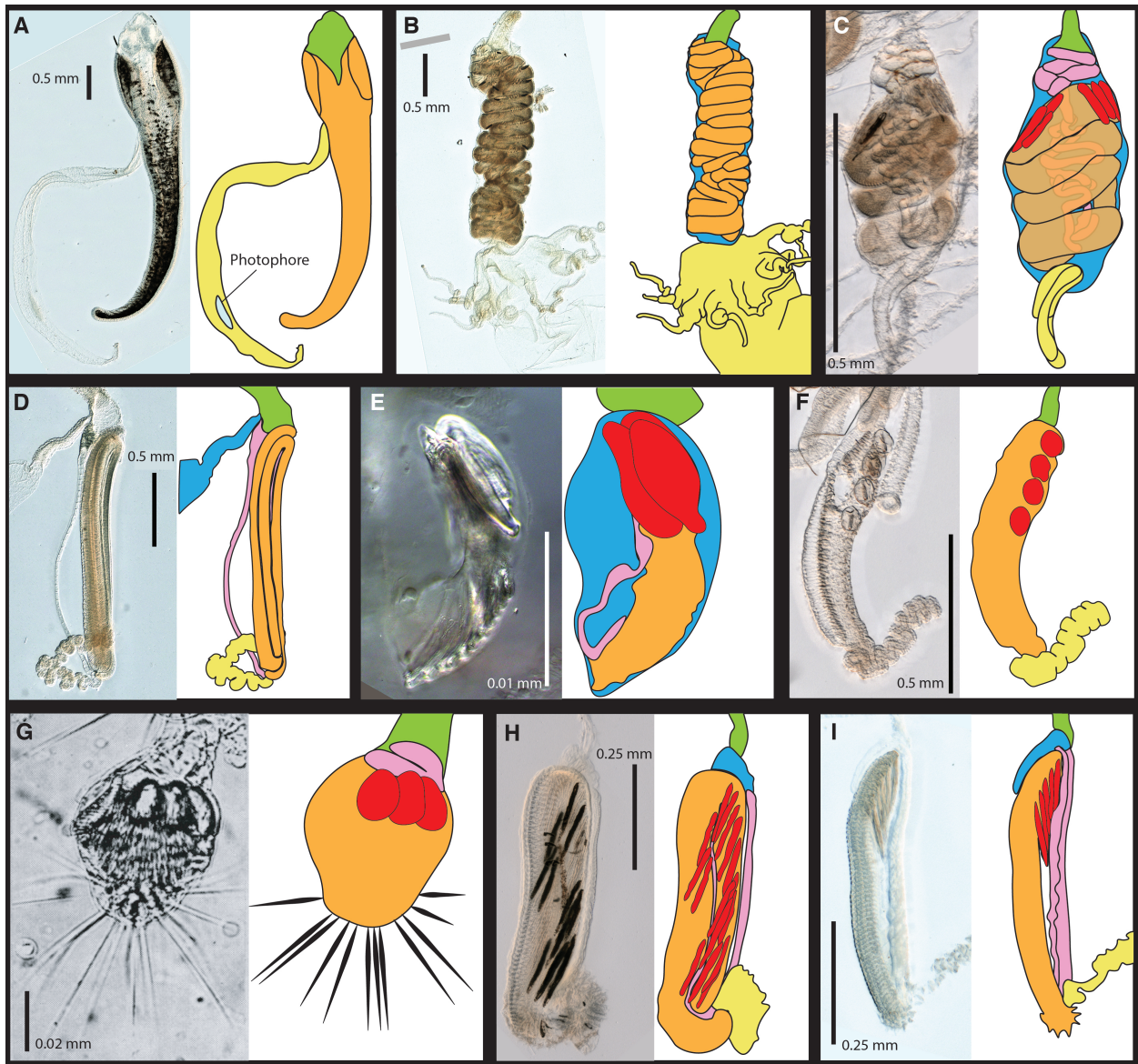


Figure 1: Tentillum diversity. The illustrations delineate the pedicle (green), involucrum (blue), cnidoband (orange), elastic strands (pink), terminal structures (yellow). Heteroneme nematocysts (stenoteles in C,E,F,G and mastigophores in H,I) are depicted in red for some species. A - *Erenna laciniata*, 10x. B - *Lychnagalma utricularia*, 10x. C - *Agalma elegans*, 10x. D - *Resomia ornicephala*, 10x. E - *Frillagalma vityazi*, 20x. F - *Bargmannia amoena*, 10x. G - *Cordagalma* sp., reproduced from Carré 1968. H - *Lilyopsis fluoracantha*, 20x. I - *Abylopsis tetragona*, 20x.

51 work we present here is complementary to (14), showcasing a far more detailed account on
52 the evolutionary history of tentilla morphology.

53 Nematocysts are unique biological weapons for defense and prey capture exclusive to the
54 phylum Cnidaria. Mariscal ((15)) reported that hydrozoans have the largest diversity of
55 nematocyst types among cnidarians. Among them, siphonophores present the greatest variety
56 of types (12), and vary widely across taxa in which and how many types they carry on their
57 tentacles. While recent descriptive studies have expanded and confirmed our understanding
58 of this diversity, the evolutionary history of nematocyst type gain and loss in siphonophores
59 remains unexplored. Thus, here we reconstruct the evolution of shifts, gains, and losses of
60 nematocyst types, subtypes, and other major categorical traits that led to the extant diversity
61 we see in siphonophore tentilla. In (14), we found strong associations between piscivory
62 and haploneme shape. These associations could have been produced by convergent changes
63 in the adaptive optima of these characters. Here we set out to test this hypothesis using
64 comparative model fitting methods. Analyzing the diversity of morphological states from a
65 phylogenetic perspective allows us to identify the specific evolutionary processes that gave
66 rise to it. Here we fit and compare a variety of macroevolutionary models to siphonophore
67 tentilla morphology measurement data to identify instances of neutral divergence, stabilizing
68 selection, changes in the speed of evolution, convergent evolution, and paedomorphosis (larval
69 characters present in mature colonies).

70 In (14) we fitted discriminant analyses to identify characters that are predictive of feeding
71 guild. These discriminant analyses can be used to generate hypotheses on the diets of
72 ecologically understudied siphonophore species for which we have morphology data. Here
73 we present a Bayesian prediction for the feeding guild of 45 species using the morphological
74 dataset in (14). As mentioned above, tentilla are far from being ornamental shapes and are
75 in fact violently reactive weapons for prey capture (14, 16). While we now have detailed
76 characterizations of tentilla morphologies across many species, the diversity of dynamic
77 performances and their relationships to the undischarged morphologies have not been examined

78 to date. To address this gap, we set out to record high-speed video of the *in vivo* discharge
79 dynamics of several siphonophore species at sea, and compare the kinematic attributes to
80 their morphological characters.

81 Methods

82 All character data and the phylogeny analyzed here were published in (14). We log transformed
83 all the continuous characters that did not pass Shapiro-Wilks normality tests, and used
84 the ultrametric constrained Bayesian time tree in all comparative analyses. When missing
85 data was incorporated as inapplicable states, we removed those species with characters that
86 could not be measured due to technical limitations. We used the feeding guild categories
87 detailed in (14) with one modification: including all *Forskalia* spp. as generalists not only
88 a single *Forskalia* species on the tree after a reinterpretation of the data in (17). In order
89 to characterize the evolutionary history of tentilla morphology, we fitted different models
90 generating the observed data distribution given the phylogeny for each continuous character
91 using the function `fitContinuous` in the R package *geiger* (18). These models include a
92 non-phylogenetic white-noise model (WN), a neutral divergence Brownian Motion model
93 (BM), an early-burst decreasing rate model (EB), and an Ornstein-Uhlenbeck (OU) model
94 with stabilizing selection around a fitted optimum trait value. In the same way as (14) we
95 then ordered the models by increasing parametric complexity (WN, BM, EB, OU), and
96 compared their corrected Akaike Information Criterion (AICc) scores (19). We used the
97 lowest (best) score using a delta cutoff of 2 units to determine significance relative to the
98 next simplest model (SM10). We calculated model adequacy scores using the R package
99 *arbutus* (20) (SM11). We calculated phylogenetic signals in each of the measured characters
100 using Blomberg's K (21) (SM10). To reconstruct the ancestral character states of nematocyst
101 types and other categorical traits, we use stochastic character mapping (SIMMAP) using the
102 package *phytools* (22).

103 In order to examine the phenotypic integration in the tentillum, we explored the correla-

104 tional structure among continuous characters and among their evolutionary histories using
105 principal component analysis (PCA) and phylogenetic PCA (22). Since the character dataset
106 contains many gaps due to missing characters and inapplicable states, we carried out these
107 analyses on a subset of species and characters that allowed for the most complete dataset.
108 This was done by removing the terminal filament characters (which are only shared by a small
109 subset of species), and then removing species which had inapplicable states for the remaining
110 characters (apolemiids and cystonects). In addition, we obtained the correlations between
111 the phylogenetic independent contrasts (23) using the package *rphylip* (24). We identified
112 four hypothetical modules among the tentillum characters: (1) The tentillum scaffold module
113 – cnidoband length & width, nematocyst row number, pedicle & elastic strand width, tentacle
114 width; (2) the heteroneme module – heteroneme length & width, shafts length & width; (3)
115 the haploneme module – length and width; and (4) the terminal filament module – desmoneme
116 & rhopaloneme length & width. To test and quantify phenotypic integration between these
117 multivariate modules, we used the phylogenetic phenotypic integration test in the package
118 *geomorph* (25).

119 When looking at the morphospace of species in different feeding guilds, we also used
120 PCA on the complete tentacular character dataset transforming inapplicable states of absent
121 characters to zeros to account for similarity based on character presence/absence. Using
122 these principal components, we examined the occupation of the morphospace across species
123 in different feeding guilds using a phylogenetic MANOVA with the package *geiger* (18) to
124 assess the variation explained, and a morphological disparity test with the package *geomorph*
125 (25) to assess differences in the extent occupied by each guild.

126 In order to detect and evaluate instances of convergent evolution, we used the package
127 SURFACE (26). This tool identifies OU regimes and their optima given a tree and character
128 data, and then evaluates where the same regime has appeared independently in different
129 lineages. We applied these analyses to the haploneme nematocyst length and width characters
130 as well as to the most complete dataset without inapplicable character states.

₁₃₁ In order to generate hypotheses on the diets of siphonophores using tentilla morphology,
₁₃₂ we used the discriminant analyses of principal components (DAPC) (27) trained in (14) to
₁₃₃ predict the feeding guilds of species in the dataset for which there are no published feeding
₁₃₄ observations.

₁₃₅ In order to observe the discharge behavior of different tentilla, we recorded high speed
₁₃₆ footage (1000-3000 fps) of tentillum and nematocyst discharge by live siphonophore specimens
₁₃₇ (26 species) using a Phantom Miro 320S camera mounted on a stereoscopic microscope. We
₁₃₈ mechanically elicited tentillum and nematocyst discharge using a fine metallic pin. We used
₁₃₉ the Phantom PCC software to analyze the footage. For the 10 species recorded, we measured
₁₄₀ total cnidoband discharge time (ms), heteroneme filament length (μm), and discharge speeds
₁₄₁ (mm/s) for cnidoband, heteronemes, haplonemes, and heteroneme shafts when possible (data
₁₄₂ available in the Dryad repository).

₁₄₃ Results

₁₄₄ *Evolutionary history of tentillum morphology* – In (14), we produced the most speciose
₁₄₅ siphonophore molecular phylogeny to date, while incorporating the most recent findings
₁₄₆ in siphonophore deep node relationships. This phylogeny revealed for the first time that
₁₄₇ the genus *Erenna* is the sister to *Stephanomia amphytridis*. *Erenna* and *Stephanomia* bear
₁₄₈ the largest tentilla among all siphonophores, thus their monophyly indicates that there was
₁₄₉ a single evolutionary transition to giant tentilla. Siphonophore tentilla range in size from
₁₅₀ $\sim 30 \mu\text{m}$ in some *Cordagalma* specimens to 2-4 cm in *Erenna* species, and up to 8 cm in
₁₅₁ *Stephanomia amphytridis* (10). Most siphonophore tentilla measure between 175 and 1007
₁₅₂ μm (1st and 3rd quartiles), with a median of 373 μm . The extreme gain of tentillum size in
₁₅₃ this newly found clade may have important implications for access to large prey size classes
₁₅₄ such as adult deep-sea fishes.

₁₅₅ Siphonophore tentilla are defined as lateral, monostichous evaginations of the tentacle
₁₅₆ gastrovascular lumen with epidermal nematocysts (11). The buttons on *Physalia* tentacles

157 were not traditionally regarded as tentilla, but (8) and our observations (13), confirm
158 that the buttons contain evaginations of the gastrovascular lumen, thus satisfying all the
159 criteria for the definition. In this light, and given that most Cystonectae bear conspicuous
160 tentilla, we conclude (in agreement with (13) and (14)) that tentilla are likely ancestral to
161 all siphonophores, and secondarily lost twice, once in *Apolemia* and again in *Bathyphysa*
162 *conifera*.

163 In order to gain a broad perspective on the evolutionary history of tentilla, we reconstructed
164 the phylogenetic positions of the main categorical character shifts using stochastic character
165 mapping (SM1-9) and summarized in (Fig. 2). Some of these characters include the gain
166 and loss of nematocyst types. Based on external information, we assume that haploneme
167 nematocysts are ancestrally present in siphonophore tentacles since they are present in the
168 tentacles of many other hydrozoans (15). Haplonemes first diverged into spherical isorhizas
169 of 2 size classes in Cystonectae, and elongated anisorhizas of one size class in Codonophora.
170 Haplonemes were likely lost in the tentacles of *Apolemia* but retained as spherical isorhizas in
171 other *Apolemia* tissues (28). Similarly, while heteronemes exist in other tissues of cystonects,
172 they appear in the tentacles of codonophorans exclusively, as birhopaloids in *Apolemia*,
173 stenoteles in eucladophoran physonects, and microbasic mastigophores in calycophorans.

174 The clades defined in (14) are characterized by unique evolutionary innovations in their
175 tentilla. The clade Eucladophora (containing Pyrostephidae, Euphysonectae, and Caly-
176 cophorae) encompasses all of the extant Siphonophore species (178 of 186) except Cystonects
177 and *Apolemia*. Innovations that arose along the stem of this group include spatially seg-
178 regated heteroneme and haploneme nematocysts, terminal filaments, and elastic strands
179 (Fig. 2). Pyrostephids evolved a unique bifurcation of the axial gastrovascular canal of
180 the tentillum known as the “saccus” (11). The stem to the clade Tendiculophora (clade
181 containing Euphysonectae and Calycophorae) subsequently acquired further novelties such
182 as the desmoneme and rhopaloneme (acrophore subtype ancestral) nematocysts on the
183 terminal filament (Fig. 2), which bears no other nematocyst type. These are arranged

184 in sets of 2 parallel rhopalonemes for each single desmoneme (29, 30). The involucrum is
185 an expansion of the epidermal layer that can cover part or all of the cnidoband (Fig. 1).
186 This structure, together with differentiated larval tentilla, appeared in the stem branch to
187 Clade A physonects. Calycophorans evolved novelties such as larger desmonemes at the
188 distal end of the cnidoband, pleated pedicles with a “hood” (here considered homologous
189 to the involucrum) at the proximal end of the tentillum, anacrophore rhopalonemes, and
190 microbasic mastigophore-type heteronemes. While calycophorans have diversified into most
191 of the extant described siphonophore species (108 of 186), their tentilla have not undergone
192 any major categorical gains or losses since their most recent common ancestor. Nonetheless,
193 they have evolved a wide variation in nematocyst and cnidoband sizes. Ancestrally (and
194 retained in most prayomorphs and hippopodids), the calycophoran tentillum is recurved
195 where the proximal and distal ends of the cnidoband are close together. Diphyomorph tentilla
196 are slightly different in shape, with straighter cnidobands.

197 *Evolution of tentillum and nematocyst characters* – One-third of the characters measured
198 in (14) support a non-phylogenetic generative model, indicating they are not phylogenetically
199 conserved (SM10). Most (74%) characters present a significant phylogenetic signal, yet only
200 total nematocyst volume, haploneme length, and heteroneme-to-cnidoband length ratio had
201 a phylogenetic signal with K larger than 1. Total nematocyst volume and cnidoband-to-
202 heteroneme length ratio showed strongly conserved phylogenetic signals. The majority (67%)
203 of characters support BM models, indicating a history of neutral constant divergence. We did
204 not find any relationship between phylogenetic signal and BM model support. Haploneme
205 nematocyst length was the only character with support for an EB model of decreasing rate
206 of evolution with time. No character had support for a single-optimum OU model (when not
207 informed by feeding guild regime priors). The model adequacy tests (SM11) indicate that
208 many characters may have a relationship between the states and the rates of evolution (Sasr)
209 not captured in the basic models compared here, accompanied by a signal of unaccounted
210 rate heterogeneity (Cvar). No characters show significant deviations in the overall rate of

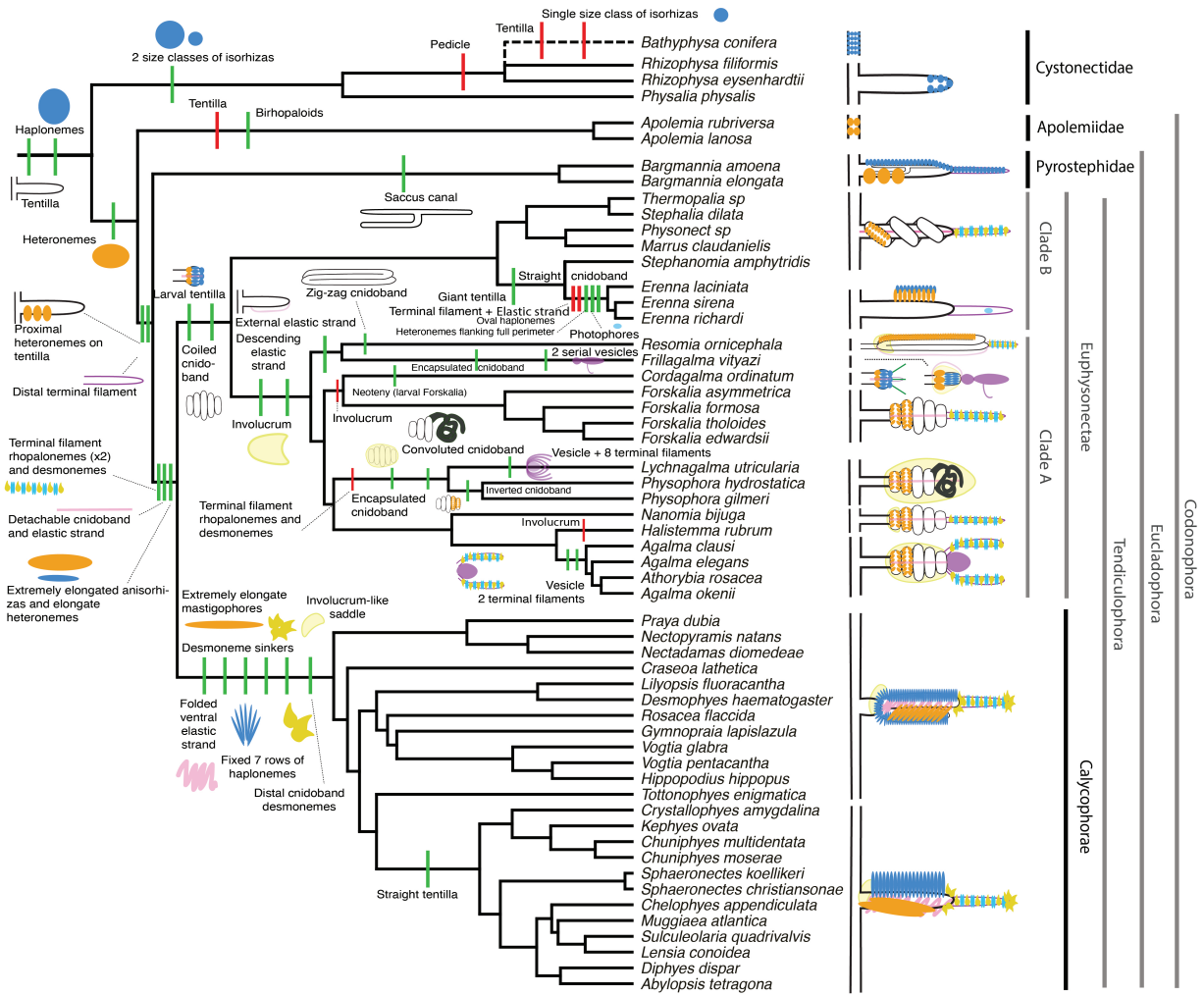


Figure 2: Siphonophore cladogram with the main categorical character gains (green) and losses (red) mapped. Some branch lengths were modified from the Bayesian chronogram to improve readability. The main visually distinguishable tentillum types are sketched next to the species that bear them, showing the location and arrangement of the main characters. In large, complex-shaped euphysonect tentilla, haplonemes were omitted for simplification. The hypothesized phylogenetic placement of the rhizophysid *Bathyphysa conifera* branch was appended manually as a polytomy (dashed line).

evolution estimated (Msig). Some characters show a perfect fit (no significant deviations across all metrics) under BM evolution, such as heteroneme shape, length, width & volume, haploneme width & SA/V, tentacle width and pedicle width. Haploneme row number and rhopaloneme shape have significant deviations across four metrics, indicating that BM (best model) is a poor fit. These characters likely evolved under complex models which would require many more data points than we have available to fit with accuracy.

Evolution of nematocyst shape – The greatest evolutionary change in haploneme nematocyst shape occurred in a single shift towards elongation in the stem of Tendiculophora, which contains the majority of described siphonophore species other than Cystonects, *Apolemia*, and Pyrostephidae. There is one secondary return to more oval, less elongated haplonemes in *Erenna*, but it does not reach the sphericity present in Cystonectae or Pyrostephidae (Fig. 4). Heteroneme evolution presents a less discrete evolutionary history, where Tendiculophora evolved more elongate heteronemes, but the difference between theirs and other siphonophores is much smaller than the variation in shape within Tendiculophora, bearing no phylogenetic signal. In this clade, the evolution of heteroneme shape has diverged in both directions, and there is no correlation with haploneme shape (Fig. 4), which has remained fairly constant (elongation between 1.5 and 2.5). Haploneme and heteroneme shape share 21% of their variance across extant values, and 53% of the variance in their shifts along the branches of the phylogeny. However, much of this correlation is due to the sharp contrast between Pyrostephidae and their sister group Tendiculophora. We searched for regime shifts in the evolution of haploneme nematocyst shape characters using a SURFACE (26). SURFACE identified seven distinct OU regimes in the evolutionary history of haploneme length and width (Fig. 7A). The different regimes are located (1) in cystonects, (2) in pyrostephids, (7) in apolemiids, (9) in *Erenna*, (6) in *Stephanomia*, (3) in most of Tendiculophora, (5) in *Cordagalma ordinatum*, (4) in most diphyomorphs, and (8) in *Abylopsis tetragona* and *Diphyes dispar*.

Phenotypic integration of the tentillum – Phenotypically integrated structures maintain

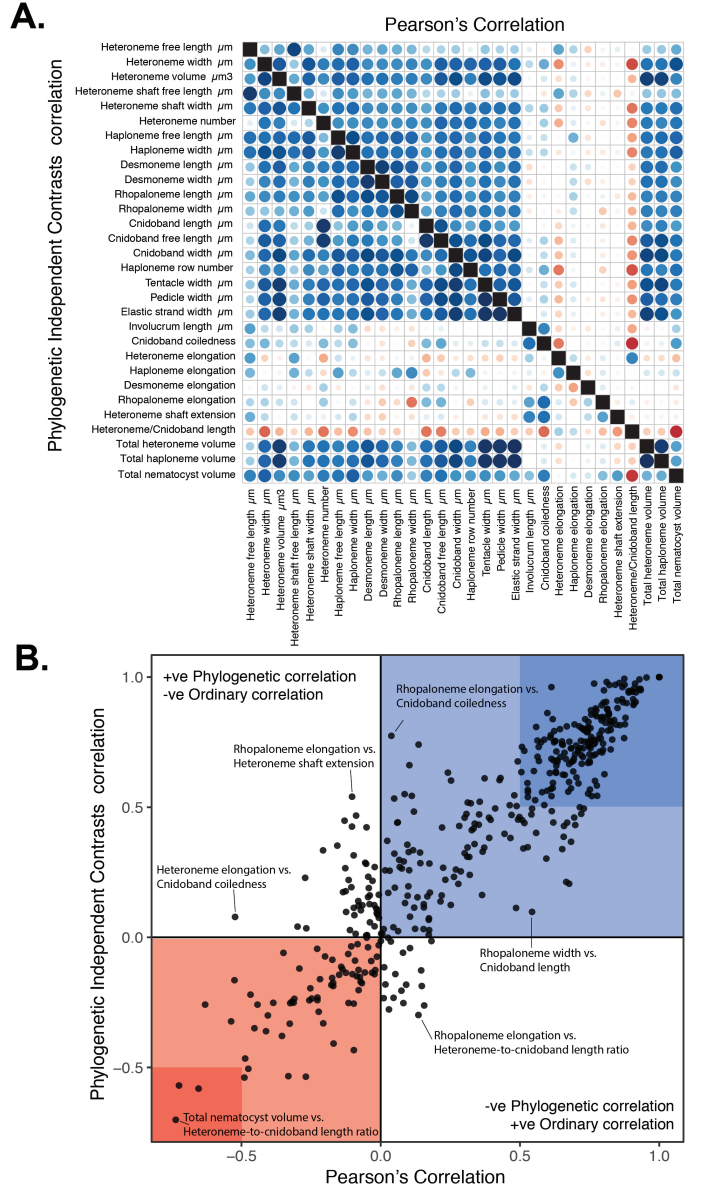


Figure 3: A. Correlogram showing strength of ordinary (upper triangle) and phylogenetic (lower triangle) correlations between characters. Both size and color of the circles indicate the strength of the correlation (R^2). B. Scatterplot of phylogenetic correlation against ordinary correlation showing a strong linear relationship ($R^2 = 0.92$, 95% confidence between 0.90 and 0.93). Light red and blue boxes indicate congruent negative and positive correlations respectively. Darker red and blue boxes indicate strong (<-0.5 or >0.5) negative and positive correlation coefficients respectively.

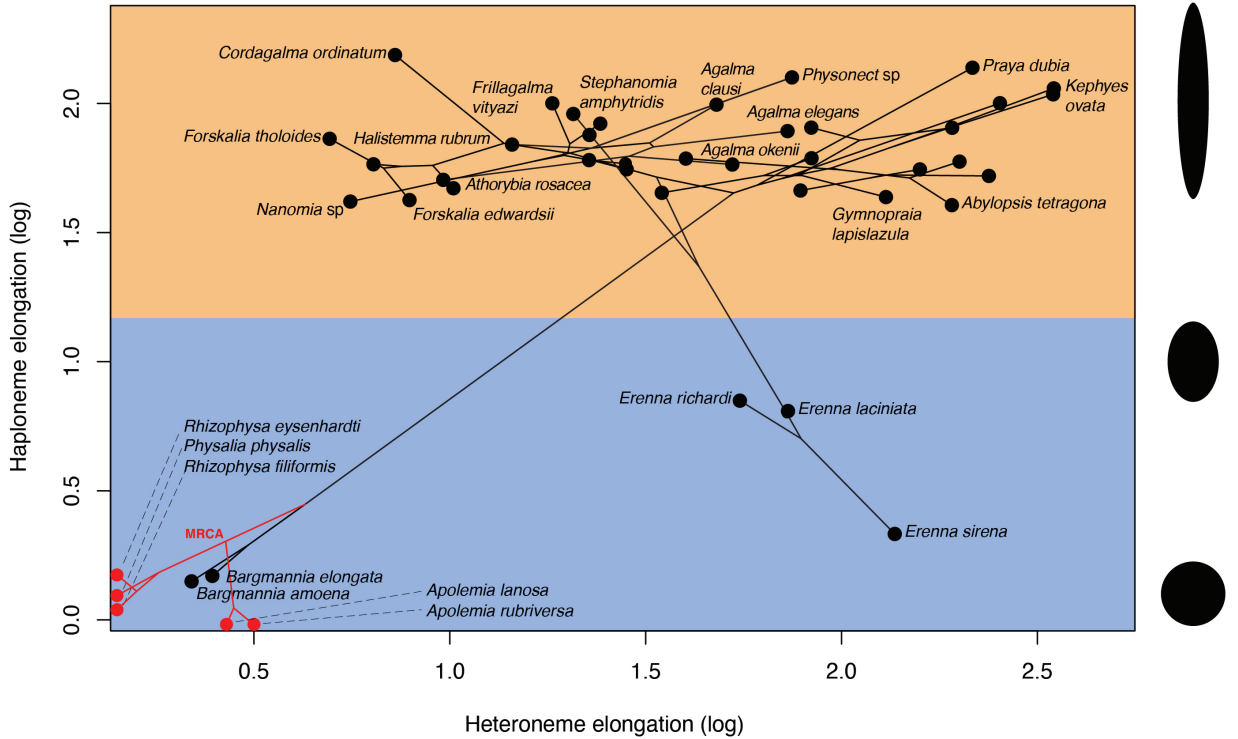


Figure 4: Phylomorphospace showing haploneme and heteroneme elongation (log scaled). Orange area delimits rod-shaped haplonemes, the blue area covers oval and round-shaped haplonemes. Smaller dots and lines represent phylogenetic relationships and ancestral states of internal nodes under BM. Species nodes in red lack either haplonemes or heteronemes, and their values are projected onto the axis of the nematocyst type they bear. Cystonects have no tentacle heteronemes and are projected onto the haploneme axis. Apolemiids have no tentacle haplonemes and are projected onto the heteroneme axis.

evolutionary correlations between its constituent characters. Of the phylogenetic correlations (Fig. 3a, lower triangle), 81.3% were positive and 18.7% were negative, while of the ordinary correlations (Fig. 3a, upper triangle) 74.6% were positive and 25.4% were negative. Half (49.9%) of phylogenetic correlations were >0.5 , while only 3.6% are < -0.5 . Similarly, among the correlations across extant species, 49.1% were >0.5 and only 1.5% were < -0.5 . In addition, we found that 13.9% of character pairs had opposing phylogenetic and ordinary correlation coefficients. Just 4% have negative phylogenetic and positive ordinary correlations (such as rhopaloneme elongation \sim heteroneme-to-cnidoband length ratio and haploneme elongation, or haploneme elongation \sim heteroneme number), and only 9.9% of character pairs had positive phylogenetic correlation yet negative ordinary correlation (such as heteroneme elongation \sim cnidoband convolution and involucrum length, or rhopaloneme elongation with cnidoband length). These disparities could be explained by Simpson's paradox (31): the reversal of the sign of a relationship when a third variable (or a phylogenetic topology (32)) is considered. However, no character pair had correlation coefficient differences larger than 0.64 between ordinary and phylogenetic correlations (heteroneme shaft extension \sim rhopaloneme elongation has a Pearson's correlation of 0.10 and a phylogenetic correlation of -0.54). Rhopaloneme elongation shows the most incongruencies between phylogenetic and ordinary correlations with other characters. The phenotypic integration test showed significant integration signal between all modules, tentillum and haploneme modules sharing the greatest regression coefficient (SM12).

In the non-phylogenetic PCA morphospace using only simple characters (Fig. 5), PC1 (aligned with tentillum and tentacle size) explained 69.3% of the variation in the tentillum morphospace, whereas PC2 (aligned with heteroneme length, heteroneme number, and haploneme arrangement) explained 13.5%. In a phylogenetic PCA, 63% of the evolutionary variation in the morphospace is explained by PC1 (aligned with shifts in tentillum size), while 18% is explained by PC2 (aligned with shifts in heteroneme number and involucrum length).

Morphospace occupation – In order to examine the occupation structure of the morphospace

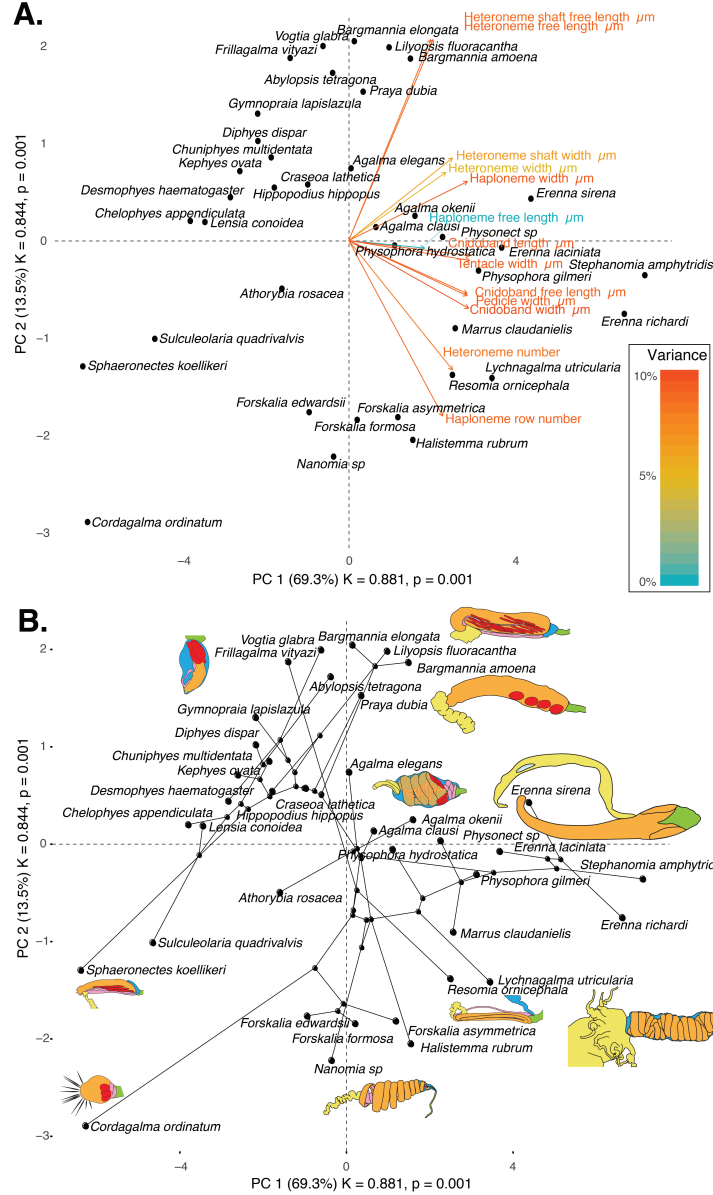


Figure 5: Phylomorphospace of the simple continuous characters principal components, excluding ratios and composite characters. A. Variance explained by each variable in the PC1-PC2 plane. Axis labels include the phylogenetic signal (K) for each component and p-value. B. Phylogenetic relationships between the species points distributed in that same space.

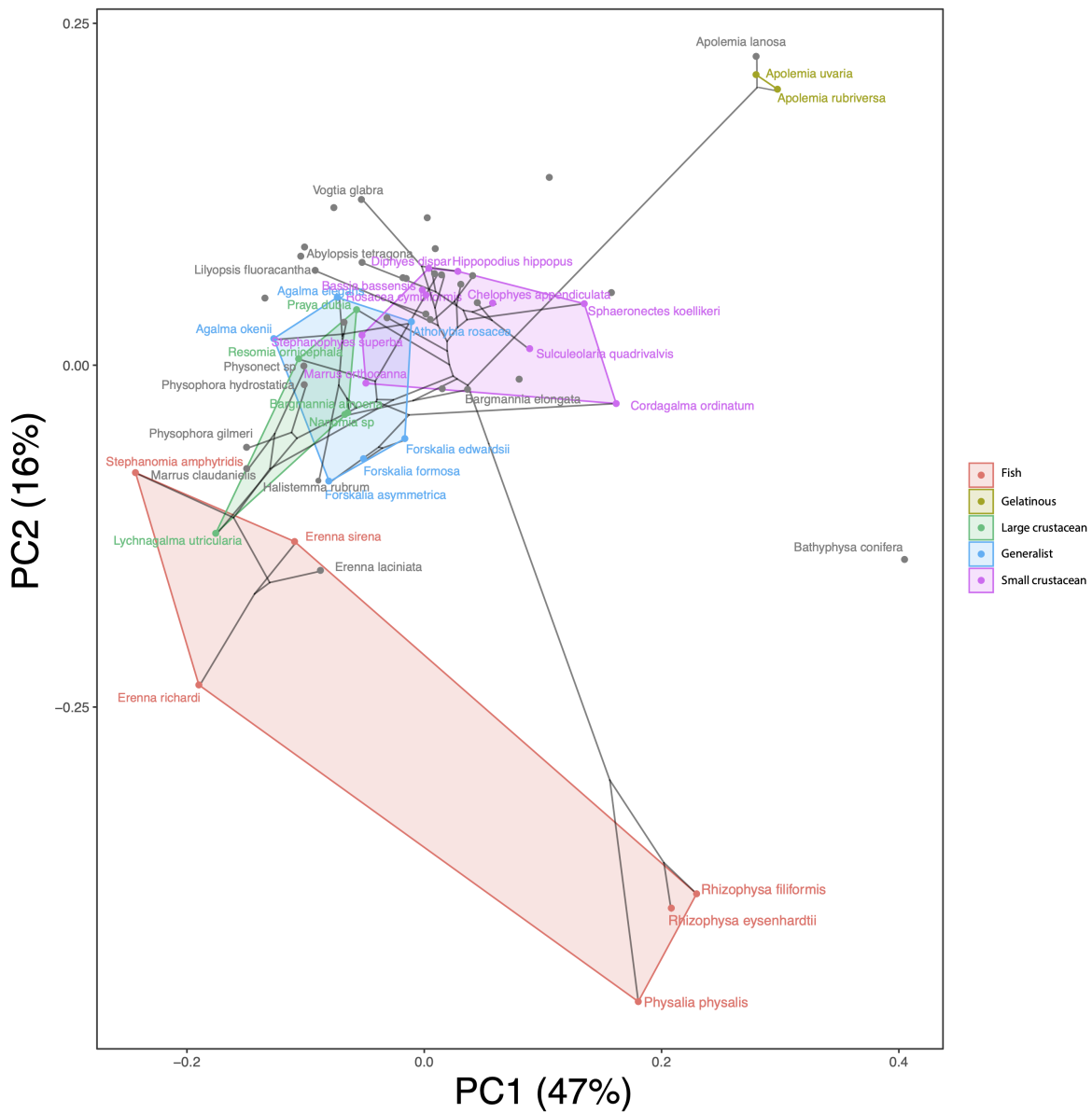


Figure 6: Phylomorphospace showing PC1 and PC2 from a PCA of continuous morphological characters with inapplicable states transformed to zeroes, overlapped with polygons conservatively defining the space occupied by each feeding guild. Lines between species coordinates show the phylogenetic relationships between them.

across all siphonophore species in the dataset, we cast a PCA on the data after transforming inapplicable states (due to absence of character) to zeroes. This allows us to accommodate species with many missing characters (such as cystonects or apolemiids), and to account for common absences as morphological similarities. In this ordination, PC1 explains 47.45% of variation (aligned with cnidoband size) and PC2 explains 16.73% of variation (aligned with heteroneme volume and involucrum). When superimposing feeding guilds onto the morphospace (Fig. 6), we find that the morphospaces of each feeding guild are only slightly overlapping in PC1 and PC2. A phylogenetic MANOVA showed that feeding guilds explain 27.63% of variance across extant species (p value < 0.000001), and 20.97% of the variance in the tree species accounting for phylogeny, an outcome significantly distinct from the expectation under neutral evolution (p -value = 0.0196). In addition, a morphological disparity analysis accounting for phylogenetic structure shows that the morphospace of fish specialists is significantly broader than that of generalists and other specialists. This is due to the large morphological disparities between cystonects and piscivorous euphysonects. There are no significant differences among the morphospace disparities of the other feeding guilds.

Convergent evolution – Convergence is a widespread evolutionary phenomenon where distantly related clades independently evolve similar phenotypes. Using the package SURFACE (26), we identified convergence in haploneme nematocyst shape and in morphospace position. In (14), we identified haploneme nematocyst shape as one of the traits associated with the convergent evolution of piscivory. Here we find that indeed wider haploneme nematocysts have convergently evolved in the piscivore cytonects and *Erenna* spp. (Fig. 7A). Extremely narrow haplonemes have also evolved convergently in *Cordagalma ordinatum* and copepod specialist calycophorans such as *Sphaeronectes koellikeri*. When integrating many traits into a couple principal components, we find two distinct convergences between euphysonects and calycophorans with a reduced prey capture apparatus. Those convergences are between *Frillagalma vityazi* and calycophorans, and once again between *Cordagalma ordinatum* and *Sphaeronectes koellikeri* (Fig. 7B).

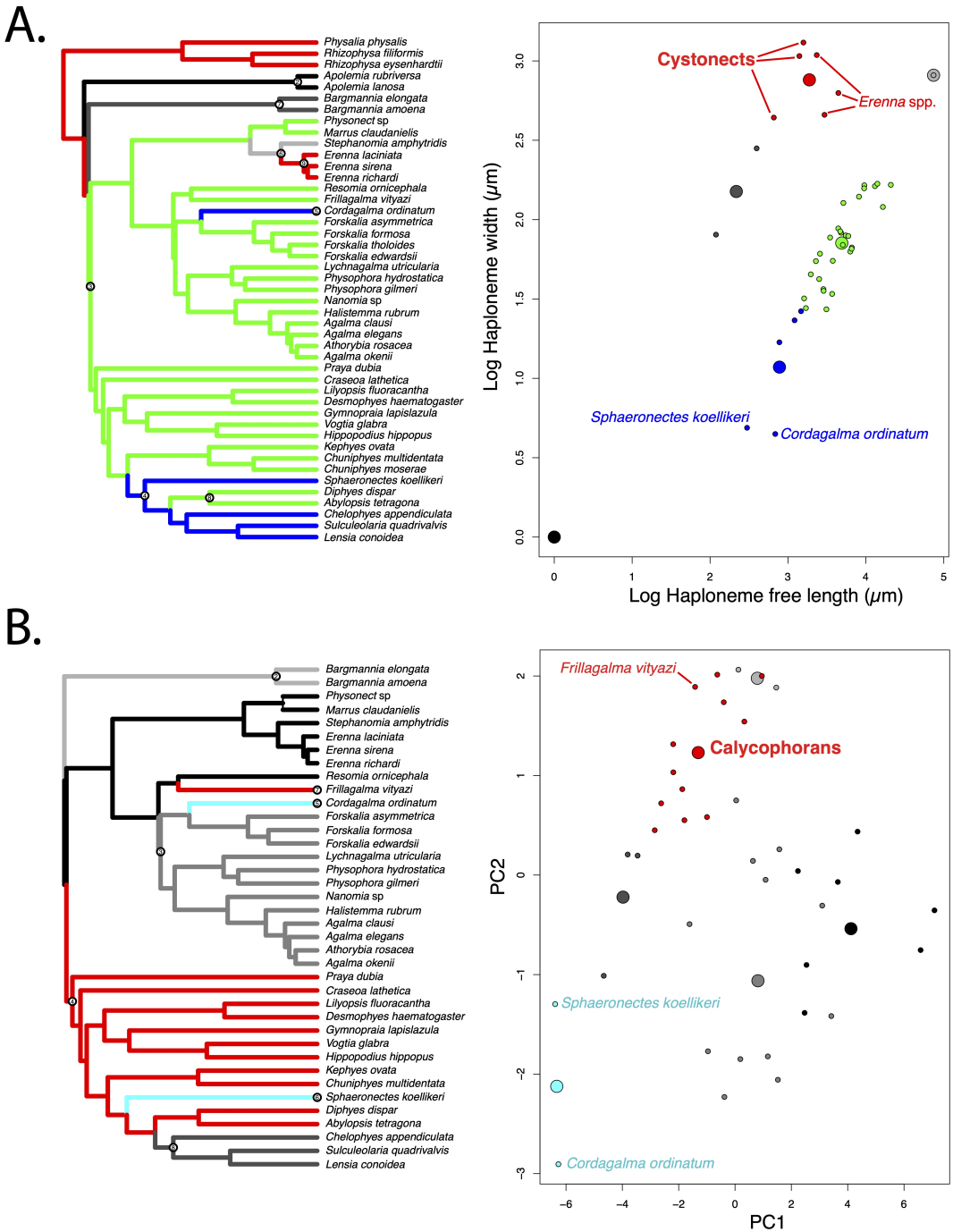


Figure 7: SURFACE plots showing convergent evolutionary regimes modelled under OU for (A) haploneme nematocyst length & width, and (B) for PC1 & 2 of all continuous characters with the exception of terminal filament nematocysts, and removing taxa with inapplicable character states. Node numbers on the tree label different regimes, regimes of the same color are identified as convergent. Small circles on the scatterplots indicate species values, large circles indicate the average position of the OU optima (θ) for a given combination of convergent regimes.

292 *Functional morphology of tentillum and nematocyst discharge* – Tentillum and nematocyst
293 discharge high speed measurements are available in the Dryad repository. While the sample
294 sizes of these measurements were insufficient to draw reliable statistical results at a phyloge-
295 netic level, we did observe patterns that may be relevant to their functional morphology. For
296 example, cnidoband length is strongly correlated with discharge speed (p value = 0.0002).
297 This is probably the sole driver of the considerable difference between euphysonect and
298 calycophoran tentilla discharge speeds (average discharge speeds: 225.0mm/s and 41.8mm/s
299 respectively; t-test p value = 0.011), since the euphysonects have larger tentilla than the
300 calycophorans among the species recorded. In addition, we observed that calycophoran
301 haploneme tubules fire faster than those of euphysonects (T-test p value = 0.001). Haploneme
302 nematocysts discharge 2.8x faster than heteroneme nematocysts (T-test p value = 0.0012).
303 Finally, we observed that the stenoteles of the Euphysonectae discharge a helical filament
304 that “drills” itself through the medium it penetrates as it everts.

305 *Generating dietary hypotheses using tentillum morphology* – For many siphonophore species,
306 no feeding observations have yet been published. To help bridge this gap of knowledge,
307 we generated hypotheses about the diets of these understudied siphonophores based on
308 their known tentacle morphology using one the linear discriminant analyses of principal
309 components (DAPC) fitted in (14). This provides concrete predictions to be tested in
310 future work and helps extrapolate our findings to many poorly known species that are
311 extremely difficult to collect and observe. The discriminant analysis for feeding guild (7
312 principal components, 4 discriminants) produced 100% discrimination, and the highest loading
313 contributions were found for the characters (ordered from highest to lowest): Involutrum
314 length, heteroneme volume, heteroneme number, total heteroneme volume, tentacle width,
315 heteroneme length, total nematocyst volume, and heteroneme width. We used the predictions
316 from this discriminant function to generate hypotheses about the feeding guild of 45 species
317 in the morphological dataset. This extrapolation predicts that two other *Apolemia* species are
318 gelatinous prey specialists like *Apolemia rubriversa*, and predicts that *Erenna laciniata* is a

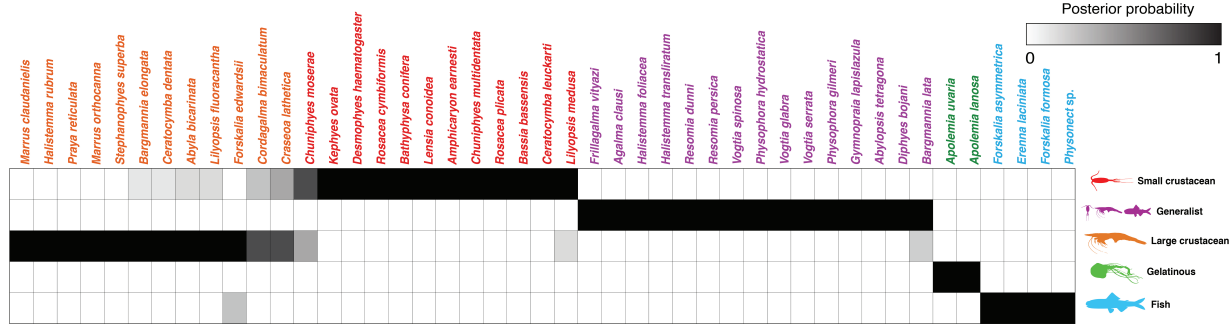


Figure 8: Hypothetical feeding guilds for siphonophore species predicted by a 6 PCA DAPC. Cell darkness indicates the posterior probability of belonging to each guild. Training data set transformed so inapplicable states are computed as zeroes. Species ordered and colored according to their predicted feeding guild.

319 fish specialist like *Erenna richardi*. When predicting soft- and hard-bodied prey specialization,
 320 the DAPC achieved 90.9% discrimination success, only marginally confounding hard-bodied
 321 specialists with generalists (SM13). The main characters driving this discrimination are
 322 involucrum length, heteroneme number, heteroneme volume, tentacle width, total nematocyst
 323 volume, total haploneme volume, elastic strand width, and heteroneme length.

324 Discussion

325 *On the evolution of tentilla morphology – On the evolution of tentilla morphology –* The
 326 evolutionary rate covariance results in (14) indicate that tentilla are not only phenotypically
 327 integrated but also show patterns of evolutionary modularity, where different sets of characters
 328 appear to evolve in stronger correlations among each other than with other characters (33).
 329 This may be indicative of the underlying genetic and developmental dependencies among
 330 closely homologous nematocyst types (such as desmonemes and rhopalonemes) and structures.
 331 The rate covariance results are congruent with the evolutionary correlations we found (Fig.
 332 ??figure8)). In addition, these evolutionary modules point to hypothetical functional modules.
 333 For example, the coiling degree of the cnidoband and the extent of the involucrum have
 334 correlated rates of evolution, while high-speed videos (pers. obs.) show that the involucrum
 335 helps direct the whiplash of the uncoiling cnidoband distally (towards the prey). The clade

³³⁶ Tendiculophora contains far more species than its relatives Cystonectae, Apolemiidae, and
³³⁷ Pyrostephidae. An increase in clade richness and ecological diversification can be triggered
³³⁸ by a ‘key innovation’ (34). The evolutionary innovation of the Tendiculophora tentilla with
³³⁹ shooting cnidobands and modular regions may have facilitated further dietary diversification.
³⁴⁰ A specific instance of this may have been the access to the abundant small crustacean prey
³⁴¹ such as copepods. The rapid darting escape response of copepods may preclude their capture
³⁴² in siphonophores without shooting cnidobands.

³⁴³ The siphonophore tentillum morphospace has a fairly low extant dimensionality due
³⁴⁴ to having an evolutionary history with many synchronous, correlated changes. This is
³⁴⁵ consistent with strong phenotypic integration where genetic and developmental correlations
³⁴⁶ are maintained by natural selection to preserve a complex function across the wide variety
³⁴⁷ of morphologies present. Since most tentillum characters develop from a common bud
³⁴⁸ (budding tentilla near the base of the tentacle), structural correlations are expected. Similarly,
³⁴⁹ correlations between the features of different nematocyst subtypes within a species are also
³⁵⁰ expected given their common evolutionary and developmental origin (35, 36). However, we
³⁵¹ also found correlations between nematocyst and tentillum characters. Siphonophore tentacle
³⁵² nematocysts (in their cnidocytes) are not produced nor matured in the developing tentillum.
³⁵³ These cnidocytes are produced by dividing cnidoblasts in the basigaster (basal swelling of
³⁵⁴ the gastrozooid). Once the cnidocytes have assembled the nematocyst, they migrate outward
³⁵⁵ along the tentacle (37) and position themselves in the tentillum according to their type and size
³⁵⁶ (29). Thus, the developmental programs that produce the observed nematocyst morphologies
³⁵⁷ are spatially separated from those producing the tentillum morphologies. Therefore, we
³⁵⁸ hypothesize the genetic correlations and phenotypic integration between tentillum and
³⁵⁹ nematocyst characters are maintained through natural selection on separate regulatory
³⁶⁰ networks, out of the necessity to work together and meet the spatial, mechanical, and
³⁶¹ functional constraints of their prey capture behavior.

³⁶² *Heterochrony and convergence in the evolution of tentilla with diet* - In addition to

363 identifying shifts in prey type, (14) revealed the specific morphological changes in the prey
364 capture apparatus associated with these changes. Copepod-specialized diets have evolved
365 independently in *Cordagalma* and some calycophorans. These evolutionary transitions
366 happened together with transitions to smaller tentilla with fewer and smaller cnidoband
367 nematocysts. We found that these morphological transitions evolved convergently in these
368 taxa. Tentilla are expensive single-use structures (16), therefore we would expect that
369 specialization in small prey would beget reductions in the size of the prey capture apparatus
370 to the minimum required for the ecological performance. Such a reduction in size would
371 require extremely fast rates of trait evolution in an ordinary scenario. However, *Cordagalma*'s
372 tentilla strongly resemble the larval tentilla (only found in the first-budded feeding body of
373 the colony) of their sister genus *Forskalia*. This indicates that the evolution of *Cordagalma*
374 tentilla could be a case of paedomorphic heterochrony associated with predatory specialization
375 on smaller prey. This developmental shift may have provided a shortcut for the evolution of
376 a smaller prey capture apparatus.

377 Our work identifies yet another novel example of convergent evolution. The region of
378 the tentillum morphospace (Fig. 5 & Fig. ??surface)B) occupied by calycophorans was
379 independently (and more recently) occupied by the physonect *Frillagalma vityazi*. Like
380 calycophorans, *Frillagalma* tentilla have small C-shaped cnidobands with a few rows of
381 anisorhizas. Unlike calycophorans, they lack paired elongate microbasic mastigophores.
382 Instead, they bear exactly three oval stenoteles, and their cnidobands are followed by a
383 branched vesicle, unique to this genus. Their tentillum morphology is very different from
384 that of other related physonects, which tend to have long, coiled, cnidobands with many
385 paired oval stenoteles. Our SURFACE analysis clearly indicates a regime convergence in the
386 cnidoband morphospace between *Frillagalma* and calycophorans (Fig. 7B). Most studies on
387 calycophoran diets have reported their prey to be primarily composed of small crustaceans,
388 such as copepods or ostracods (17, 38). The diet of *Frillagalma vityazi* is unknown, but this
389 morphological convergence suggests that they evolved to capture similar kinds of prey. The

³⁹⁰ DAPCs in (14) predict that *Frillagalma* has a generalist niche with both soft and hard-bodied
³⁹¹ prey, including copepods.

³⁹² *Evolution of nematocyst shape* – A remarkable feature of siphonophore haplonemes is
³⁹³ that they are outliers to all other Medusozoa in their surface area to volume relationships,
³⁹⁴ deviating significantly from sphericity (39). This suggests a different mechanism for their
³⁹⁵ discharge that could be more reliant on capsule tension than on osmotic potentials (40), and
³⁹⁶ strong selection for efficient nematocyst packing in the cnidoband (29, 39). Our results show
³⁹⁷ that Codonophora underwent a shift towards elongation and Cystonectae towards sphericity,
³⁹⁸ assuming the common ancestor had an intermediate state. Since we know that the haplonemes
³⁹⁹ of other hydrozoan outgroups are generally spheroid, it is more parsimonious to assume that
⁴⁰⁰ cystonects are simply retaining this ancestral state. Later, we observe a return to more
⁴⁰¹ rounded (ancestral) haplonemes in *Erenna*, concurrent with a secondary gain of a piscivorous
⁴⁰² trophic niche, like that exhibited by cystonects. Our SURFACE analysis shows that this
⁴⁰³ transition to roundness is convergent with the regime occupied by cystonects (Fig. 7A).
⁴⁰⁴ Purcell (38) showed that haplonemes have a penetrating function as isorhizas in cystonects
⁴⁰⁵ and an adhesive function as anisorhizas in Tendiculophora. It is no coincidence that the two
⁴⁰⁶ clades that have converged to feed primarily on fish have also converged morphologically
⁴⁰⁷ toward more compact haplonemes. Isorhizas in cystonects are known to penetrate the skin of
⁴⁰⁸ fish during prey capture, and to deliver the toxins that aid in paralysis and digestion (41).
⁴⁰⁹ *Erenna*'s anisorhizas are also able to penetrate human skin and deliver a painful sting (4)
⁴¹⁰ (and pers. obs.), a common feature of piscivorous cnidarians like the Portuguese man-o-war
⁴¹¹ or box jellies.

⁴¹² The implications of these results for the evolution of nematocyst function are that an
⁴¹³ innovation in the discharge mechanism of haplonemes may have occurred during the main shift
⁴¹⁴ to elongation. Elongate nematocysts can be tightly packed into cnidobands. We hypothesize
⁴¹⁵ this may be a Tendiculophora lineage-specific adaptation to packing more nematocysts into a
⁴¹⁶ limited tentillum space, as suggested by (29). Thomason (39) hypothesized that smaller, more

417 spherical nematocysts, with a lower surface area to volume ratio, are more efficient in osmotic-
418 driven discharge and thus have more power for skin penetration. The elongated haplonemes
419 of crustacean-eating Tendiculophora have never been observed penetrating their crustacean
420 prey (38), and are hypothesized to entangle the prey through adhesion of the abundant
421 spines to the exoskeletal surfaces and appendages. Entangling requires less acceleration and
422 power during discharge than penetration, as it does not rely on point pressure. In fish-eating
423 cystonects and *Erenna* species, the haplonemes are much less elongated and very effective at
424 penetration, in congruence with the osmotic discharge hypothesis. Tendiculophora, composed
425 of the clades Euphysonectae and Calycophorae, includes the majority of siphonophore species.
426 Within these clades are the most abundant siphonophore species, and a greater morphological
427 and ecological diversity is found. We hypothesize that this packing-efficient haploneme
428 morphology may have also been a key innovation leading to the diversification of this clade.
429 However, other characters that shifted concurrently in the stem of this clade could have been
430 equally responsible for their extant diversity.

431 *Generating hypotheses on siphonophore feeding ecology* – One motivation for our research
432 is to understand the links between predator capture tools and their diets so we can generate
433 hypotheses about the diets of siphonophores based on morphological characteristics. Indeed,
434 our discriminant analyses were able to distinguish between different siphonophore diets
435 based on morphological characters alone. The models produced by these analyses generated
436 testable predictions about the diets of many species for which we only have morphological
437 data of their tentacles. While the limited dataset used here is informative for generating
438 tentative hypotheses, the empirical dietary data are still scarce and insufficient to cast robust
439 predictions. This reveals the need to extensively characterize siphonophore diets and feeding
440 habits. In future work, we will test these ecological hypotheses and validate these models
441 by directly characterizing the diets of some of those siphonophore species. Predicting diet
442 using morphology is a powerful tool to reconstruct food web topologies from community
443 composition alone. In many of the ecological models found in the literature, interactions

⁴⁴⁴ among the oceanic zooplankton have been treated as a black box (42). The ability to predict
⁴⁴⁵ such interactions, including those of siphonophores and their prey, will enhance the taxonomic
⁴⁴⁶ resolution of nutrient-flow models constructed from plankton community composition data.

⁴⁴⁷ **Acknowledgements**

⁴⁴⁸ This work was supported by the Society of Systematic Biologists (Graduate Student Award
⁴⁴⁹ to A.D.S.); the Yale Institute of Biospheric Studies (Doctoral Pilot Grant to A.D.S.); and
⁴⁵⁰ the National Science Foundation (Waterman Award to C.W.D., and NSF-OCE 1829835 to
⁴⁵¹ C.W.D., S.H.D.H., and C. Anela Choy). A.D.S. was supported by a Fulbright Spain Graduate
⁴⁵² Studies Scholarship.

⁴⁵³ **References**

- ⁴⁵⁴ 1. Pugh P (1983) *Benthic siphonophores: A review of the family rhodaliidai (siphonophora, physonectae)* (Royal Society).
- ⁴⁵⁶ 2. Pugh P, Harbison G (1986) New observations on a rare physonect siphonophore, lychnagalma utricularia (claus, 1879). *Journal of the Marine Biological Association of the United Kingdom* 66(3):695–710.
- ⁴⁵⁹ 3. Pugh P, Youngbluth M (1988) Two new species of prayine siphonophore (calycophorae, prayidae) collected by the submersibles johnson-sea-link i and ii. *Journal of Plankton Research* 10(4):637–657.
- ⁴⁶² 4. Pugh P (2001) A review of the genus erenna bedot, 1904 (siphonophora, physonectae). *BULLETIN-NATURAL HISTORY MUSEUM ZOOLOGY SERIES* 67(2):169–182.
- ⁴⁶⁴ 5. Hissmann K (2005) In situ observations on benthic siphonophores (physonectae: Rhodaliidae) and descriptions of three new species from indonesia and south africa. *Systematics and Biodiversity* 2(3):223–249.
- ⁴⁶⁷ 6. Haddock SH, Dunn CW, Pugh PR (2005) A re-examination of siphonophore terminology and morphology, applied to the description of two new prayine species with remarkable bio-

- 469 optical properties. *Journal of the Marine Biological Association of the United Kingdom*
470 85(3):695–707.
- 471 7. Dunn CW, Pugh PR, Haddock SH (2005) *Marrus claudanielis*, a new species of
472 deep-sea physonect siphonophore (siphonophora, physonectae). *Bulletin of Marine Science*
473 76(3):699–714.
- 474 8. Bardi J, Marques AC (2007) Taxonomic redescription of the portuguese man-of-war,
475 *physalia physalis* (cnidaria, hydrozoa, siphonophorae, cystonectae) from brazil. *Iheringia*
476 *Série Zoologia* 97(4):425–433.
- 477 9. Pugh P, Haddock S (2010) Three new species of remosiid siphonophore (siphonophora:
478 Physonectae). *Journal of the Marine Biological Association of the United Kingdom* 90(6):1119–
479 1143.
- 480 10. Pugh P, Baxter E (2014) A review of the physonect siphonophore genera *halistemma*
481 (family agalmatidae) and *stephanomia* (family stephanomiidae). *Zootaxa* 3897(1):1–111.
- 482 11. Totton AK, Bargmann HE (1965) *A synopsis of the siphonophora* (British Museum
483 (Natural History)).
- 484 12. Mapstone GM (2014) Global diversity and review of siphonophorae (cnidaria: Hydro-
485 zoa). *PLoS One* 9(2):e87737.
- 486 13. Munro C, et al. (2018) Improved phylogenetic resolution within siphonophora
487 (cnidaria) with implications for trait evolution. *Molecular Phylogenetics and Evolution*.
- 488 14. Damian-Serrano A, Haddock SH, Dunn CW (2019) The evolution of siphonophore
489 tentilla as specialized tools for prey capture. *bioRxiv*:653345.
- 490 15. Mariscal RN (1974) Nematocysts.
- 491 16. Mackie GO, Pugh PR, Purcell JE (1987) Siphonophore Biology. *Advances in Marine*
492 *Biology* 24:97–262.
- 493 17. Purcell J (1981) Dietary composition and diel feeding patterns of epipelagic
494 siphonophores. *Marine Biology* 65(1):83–90.
- 495 18. Harmon LJ, Weir JT, Brock CD, Glor RE, Challenger W (2007) GEIGER: Investi-

- 496 gating evolutionary radiations. *Bioinformatics* 24(1):129–131.
- 497 19. Sugiura N (1978) Further analysts of the data by akaike's information criterion
498 and the finite corrections: Further analysts of the data by akaike's. *Communications in*
499 *Statistics-Theory and Methods* 7(1):13–26.
- 500 20. Pennell MW, FitzJohn RG, Cornwell WK, Harmon LJ (2015) Model adequacy and the
501 macroevolution of angiosperm functional traits. *The American Naturalist* 186(2):E33–E50.
- 502 21. Blomberg SP, Garland T, Ives AR (2003) Testing for phylogenetic signal in comparative
503 data: Behavioral traits are more labile. *Evolution* 57(4):717–745.
- 504 22. Revell LJ (2012) Phytools: An r package for phylogenetic comparative biology (and
505 other things). *Methods in Ecology and Evolution* 3(2):217–223.
- 506 23. Felsenstein J (1985) Phylogenies and the comparative method. *The American*
507 *Naturalist* 125(1):1–15.
- 508 24. Revell LJ, Chamberlain SA (2014) Rphylip: An r interface for phylip. *Methods in*
509 *Ecology and Evolution* 5(9):976–981.
- 510 25. Adams DC, Collyer M, Kaliontzopoulou A, Sherratt E (2016) Geomorph: Software
511 for geometric morphometric analyses.
- 512 26. Ingram T, Mahler DL (2013) SURFACE: Detecting convergent evolution from
513 comparative data by fitting ornstein-uhlenbeck models with stepwise akaike information
514 criterion. *Methods in ecology and evolution* 4(5):416–425.
- 515 27. Jombart T, Devillard S, Balloux F (2010) Discriminant analysis of principal compo-
516 nents: A new method for the analysis of genetically structured populations. *BMC genetics*
517 11(1):94.
- 518 28. Siebert S, Pugh PR, Haddock SH, Dunn CW (2013) Re-evaluation of characters in
519 apolemiidae (siphonophora), with description of two new species from monterey bay, california.
520 *Zootaxa* 3702(3):201–232.
- 521 29. Skaer R (1988) *The formation of cnidocyte patterns in siphonophores* (Academic
522 Press New York).

- 523 30. Skaer R (1991) Remodelling during the development of nematocysts in a siphonophore.
- 524 *Hydrobiologia* (Springer), pp 685–689.
- 525 31. Blyth CR (1972) On simpson's paradox and the sure-thing principle. *Journal of the*
- 526 *American Statistical Association* 67(338):364–366.
- 527 32. Uyeda JC, Zenil-Ferguson R, Pennell MW (2018) Rethinking phylogenetic comparative
- 528 methods. *Systematic Biology* 67(6):1091–1109.
- 529 33. Wagner GP (1996) Homologues, natural kinds and the evolution of modularity.
- 530 *American Zoologist* 36(1):36–43.
- 531 34. Simpson GG (1955) *Major features of evolution* (Columbia University Press: New
- 532 York).
- 533 35. Bode H (1988) Control of nematocyte differentiation in hydra. *The Biology of*
- 534 *Nematocysts* (Elsevier), pp 209–232.
- 535 36. David CN, et al. (2008) Evolution of complex structures: Minicollagens shape the
- 536 cnidarian nematocyst. *Trends in genetics* 24(9):431–438.
- 537 37. Carré D (1972) Study on development of cnidocysts in gastrozooids of muggiaeae kochi
- 538 (will, 1844) (siphonophora, calycophora). *Comptes Rendus Hebdomadaires des Seances de*
- 539 *l'Academie des Sciences Serie D* 275(12):1263.
- 540 38. Purcell JE (1984) The functions of nematocysts in prey capture by epipelagic
- 541 siphonophores (coelenterata, hydrozoa). *The Biological Bulletin* 166(2):310–327.
- 542 39. Thomason J (1988) The allometry of nematocysts. *The Biology of Nematocysts*
- 543 (Elsevier), pp 575–588.
- 544 40. Carré D, Carré C (1980) On triggering and control of cnidocyst discharge. *Marine &*
- 545 *Freshwater Behaviour & Phy* 7(1):109–117.
- 546 41. Hessinger DA (1988) Nematocyst venoms and toxins. *The Biology of Nematocysts*
- 547 (Elsevier), pp 333–368.
- 548 42. Mitra A (2009) Are closure terms appropriate or necessary descriptors of zooplankton
- 549 loss in nutrient–phytoplankton–zooplankton type models? *Ecological Modelling* 220(5):611–

550 620.